

## Excitation Functions for Heavy-Ion-Induced Reactions on Aluminum-27\*

INGE-MARIA LADENBAUER-BELLIS,<sup>†</sup> IVOR L. PREISS, AND C. E. ANDERSON<sup>‡</sup>  
*Heavy Ion Accelerator Laboratory, Physics Department, Yale University, New Haven, Connecticut*

(Received June 21, 1961; revised manuscript received September 1, 1961)

Excitation functions for a number of  $C^{12}$ ,  $N^{14}$ , and  $O^{16}$ -induced reactions on aluminum-27 have been studied using stacked-foil techniques and the ion beams of the Yale Heavy Ion Accelerator. The yields of  $Cl^{34,38}$ ,  $P^{32}$ ,  $Al^{28,29}$ ,  $Mg^{27}$ ,  $Na^{24}$ , and  $F^{18}$  have been measured in the energy range from 10.5 to about 1 Mev per nucleon. The production of the radionuclides  $Cl^{34,38}$ ,  $P^{32}$ , and in the case of  $C^{12}$  irradiation  $Al^{28}$ , are due to evaporation processes from a compound-nucleus system, while the production of  $F^{18}$ ,  $Na^{24}$ ,  $Al^{28}$ ,  $Al^{29}$ , and  $Mg^{27}$  seems to occur by a direct-interaction mechanism. A comparison of the yields for specific radio-nuclei produced by different beams is given.

### INTRODUCTION

HEAVY-ION-INDUCED reactions on  $Al^{27}$  have been reported by several groups.<sup>1-5</sup> However, these data have been in qualitative form, concentrated in particle detection or low or poorly defined heavy-ion beam energies. The intense beam currents and the well-defined ion beam from the Yale Heavy Ion Accelerator have facilitated a more quantitative investigation of the excitation function for the formation of several residual radio nuclides resulting from  $C^{12}$ ,  $N^{14}$ , and  $O^{16}$  bombardments on  $Al^{27}$ .

The data presented make it possible to compare excitation functions for the various residual nuclei arising from direct interaction, reaction-intermediate, or compound-nucleus formation and decay in a particular projectile-target system, as well as demonstrating the relative effects of projectile structure on the different reaction mechanisms. Of particular interest are the excitation functions for radio nuclei produced by a pickup of nucleons by the target nucleus or charge exchange (exchange transfer reaction) and those in which the target nucleus is depleted by one or more nucleons or nucleon clusters.

This study has been carried out using  $C^{12}$ ,  $N^{14}$ , and  $O^{16}$  heavy-ion beams ranging in energy from approximately one to 10.5 Mev per nucleon.  $Al^{27}$  was chosen as target material because of the availability of uniform thin foils of high purity, and the ease of identification of the residual nuclei anticipated from the heavy-ion-induced reactions (i.e.,  $Cl^{34}$ ,  $Cl^{38}$ ,  $P^{32}$ ,  $Al^{28}$ ,  $Al^{29}$ ,  $Mg^{27}$ ,  $Na^{24}$ , and  $F^{18}$ ). The cross sections were calculated from the data found by following the gamma-ray decay, gross beta decay, or both. The method of target

preparation and irradiation was the usual stacked-foil technique.

### EXPERIMENTAL

Foil stacks consisting of a number of  $Al^{27}$  foils (4.56 mg/cm<sup>2</sup> in superficial density), corresponding to the range of the incident heavy-ion beams in aluminum, were irradiated for periods ranging from 15 minutes to one hour. The incident beam energies were equivalent to  $10.5 \pm 0.2$  Mev per nucleon for  $C^{12}$  (charge +5),  $N^{14}$  (charge +6), and  $O^{16}$  (charge +6), while the minimum energy observed represented energies of approximately 1 Mev per nucleon. The beam was integrated (charge integration) by use of a Faraday cup and a Cary electrometer.

At the end of each irradiation the foils were separated, mounted on aluminum disks and the gamma-ray or gross beta decay of the radionuclides formed was followed using the same methods and equipment described in an earlier paper.<sup>6</sup>

The cross sections were calculated from the corrected disintegration rates found by gamma-ray spectroscopy and/or gross beta-decay analysis in a manner similar to that previously reported by the authors.<sup>6</sup> The beam energies in a given foil were interpolated from the data of Northcliffe.<sup>7</sup>

Table I lists the observed and literature values of the gamma-ray energies and half-lives of the residual nuclei of interest. In Tables II-IV the calculated thin-target cross sections at the various heavy-ion beam energies are tabulated.

### RESULTS

The activation cross sections listed in Tables II-IV and the corresponding excitation functions (Fig. 1-4) were determined to  $\pm 30\%$  in all cases except for the yields of  $Al^{29}$ ,  $Mg^{27}$ , and the  $Cl^{34}$ - $Cl^{38}$  yields resulting from  $O^{16}$  and  $N^{14}$  bombardments. The  $Al^{29}$  and  $Mg^{27}$  cross sections given in this paper represent the upper limit of these values, while the excitation functions for the  $O^{16}$  and  $N^{14}$  yields of  $Cl^{34}$ - $Cl^{38}$  represent the total

\* This work was supported by the U. S. Atomic Energy Commission.

<sup>†</sup> On leave from the University of Vienna, Analytical Chemical Institute.

<sup>‡</sup> Present address: Missile and Space Vehicle Department, General Electric Company, Philadelphia, Pennsylvania.

<sup>1</sup> K. F. Chackett, J. H. Fremlin, and D. Walker, *Phil. Mag.* **45**, 173 (1954).

<sup>2</sup> K. F. Chackett and J. H. Fremlin, *Phil. Mag.* **45**, 735 (1954).

<sup>3</sup> V. V. Volkov, A. S. Pasiuk, and G. N. Flerov, *JETP* **33**, 595 (1957).

<sup>4</sup> W. H. Webb, H. L. Reynolds, and A. Zucker, *Phys. Rev.* **102**, 749 (1956).

<sup>5</sup> J. J. Pinajian, *Nuclear Physics*, **17**, 44 (1960).

<sup>6</sup> I. M. Ladenbauer, I. L. Preiss, and C. E. Anderson, *Phys. Rev.* **123**, 1368 (1961).

<sup>7</sup> L. Northcliffe, *Phys. Rev.* **120**, 1744 (1960).

yield of both nuclides, since no attempt was made to resolve either their gamma-ray spectra or gross beta-decay curves (similar gamma rays and half-lives) with respect to these two nuclides.

The uncertainty in beam energies in given foils is represented by the error bars plotted with the excitation function. These error bars represent the energy

loss which the heavy ion undergoes in each given Al foil. This uncertainty in energy, and the fact that no correction for beam straggling was applied to the data, may produce a "shift" in the excitation function, corresponding to a few  $\text{mg}/\text{cm}^2$  of Al, but should not affect the general shape of the excitation functions.

The shape of the excitation functions normally

TABLE I. List of residual nuclei observed formed by  $\text{C}^{12}$ ,  $\text{N}^{14}$ , and  $\text{O}^{16}$  irradiations on aluminum-27.

Isotope	Mode of decay observed	$\gamma$ -ray energy (Mev)			Half-life	
		Literature values <sup>a</sup>	Observed values	Literature values	Observed values	
Chlorine-38	$\beta^-$ , 100%	...	...	37 min	...	
Chlorine-34	$\beta^+$ , 100%	...	...	32.4 min	35 min	
Phosphorus-32	$\beta^-$ , 100%	...	...	14.5 days	14.5 days	
Aluminum-28	$\gamma$ , ...	1.78, 100%	1.78	2.3 min	2.3 min	
Aluminum-29	$\gamma$ , ...	1.28, 85%	1.28	6.6 min	6.6 min	
Magnesium-27	$\gamma$ , ...	0.843, 70%	0.84	9.5 min	9.5 min	
	...	1.015, 30%	1.0	...	...	
Sodium-24	$\beta^-$ , 100%	...	...	...	...	
	$\gamma$ , 100%	1.368, 100%	1.36	15 hr	15 hr	
	...	2.75, 100%	2.7	...	...	
Flourine-18	$\beta^+$ , 100%	...	...	1.87 hr	1.85-1.9 hr	

<sup>a</sup> D. Strominger, J. M. Hollander, and G. T. Seaborg, Revs. Modern Phys. **30**, 585 (1958); Nuclear Data Group, *Nuclear Data Sheets* (National Academy of Sciences, National Research Council, 1959).

TABLE II.  $\text{C}^{12}$ -induced reaction on  $\text{Al}^{27}$ .

Foil No.	Energy (Mev)	Formation cross section (mb)						
		$\text{Cl}^{34}$	$\text{P}^{32}$	$\text{Al}^{28}$	$\text{Al}^{29}$	$\text{Mg}^{27}$	$\text{Na}^{24}$	$\text{F}^{18}$
1	126.0-120.5	...	...	...	...	...	(13.0) <sup>a</sup>	(11.9) <sup>a</sup>
2	120.5-115.0	...	22.4	...	...	...	24.6	19.5
3	115.0-108.5	...	27.2	3.84	0.69	0.73 <sub>2</sub>	22.5	22.5
4	108.5-102.5	...	32.0	6.40	0.69	0.24 <sub>4</sub>	14.7	29.5
5	102.5- 94.8	...	41.6	...	...	...	11.2	27.2
6	94.8- 89.5	...	56.8	50.8	0.73	...	7.7 <sub>5</sub>	27.8
7	89.5- 82.4	6.0	75.3	...	...	...	4.6 <sub>3</sub>	19.8
8	82.4- 75.5	7.2	89.7	4.74	0.55	...	...	14.5
9	75.5- 66.2	5.6	99.3	...	...	...	...	14.5
10	66.2- 57.6	14.0	92.8	...	...	...	...	4.0
11	57.6- 47.5	19.0	56.0	...	...	...	...	...
12	47.5- 35.2	60.0	14.4	...	...	...	0.57	...
13	35.2- 20.4	76.0	...	...	...	...	0.38	...
14	20.4- 3.0	5.4	...	...	...	...	0.08	...
15	3.0 ...	...	...	...	...	...	0.06	...

<sup>a</sup> Values in parenthesis are not shown in the corresponding excitation functions.

TABLE III.  $\text{N}^{14}$ -induced reaction on  $\text{Al}^{27}$ .

Foil No.	Energy (Mev)	Formation cross section (mb)						
		$\text{Cl}^{34+38}$	$\text{P}^{32}$	$\text{Al}^{28}$	$\text{Al}^{29}$	$\text{Mg}^{27}$	$\text{Na}^{24}$	$\text{F}^{18}$
1	147.0-140.0	(4.8) <sup>a</sup>	(10.4) <sup>a</sup>	...	...	...	(14.3) <sup>a</sup>	(8.9) <sup>a</sup>
2	140.0-132.0	11.2	37.4	15.3	10.2	2.09	24.6	17.9
3	132.0-123.0	10.1	45.8	...	...	...	22.2	20.7
4	123.0-114.0	12.7	54.8	15.3	15.3	<1.0	21.3	20.0
5	114.0-104.0	12.0	54.8	...	...	...	20.3	20.4
6	104.0- 95.7	12.4	54.8	19.2	<1.5	<0.1	15.3	21.6
7	95.7- 87.0	15.7	45.8	...	...	...	13.2	21.6
8	87.0- 75.0	28.4	45.8	19.2	...	...	7.9	24.4
9	75.0- 63.2	36.0	65.5	...	...	...	3.0	22.3
10	63.2- 48.5	34.4	87.3	9.0	...	...	...	16.0
11	48.5- 30.8	34.4	84.5	...	...	...	...	5.5
12	30.8- 8.0	25.5	10.4	...	...	...	...	0.65
13	8.0- ...	...	...	...	...	...	...	...

<sup>a</sup> Values in parenthesis are not shown in the corresponding excitation functions.

TABLE IV.  $O^{16}$ -induced reaction on  $Al^{27}$ .

Foil No.	Energy (Mev)	Formation cross section (mb)						
		$Cl^{34+38}$	$P^{32}$	$Al^{28}$	$Al^{29}$	$Mg^{27}$	$Na^{24}$	$F^{18}$
1	168.0-161.0	(3.9) <sup>a</sup>	(8.9) <sup>a</sup>	...	...	...	(9.3) <sup>a</sup>	(11.7) <sup>a</sup>
2	161.0-150.0	8.9	45.3	8.82	present	0.59	16.2	21.7
3	150.0-140.0	8.9	58.3	6.78	in foils	0.44	15.6	27.0
4	140.0-129.0	9.6	66.5	8.14	1 to 4	...	13.4	28.1
5	129.0-114.2	9.6	81.0	5.28	...	0.15	6.7	33.9
6	114.2-104.5	10.0	93.5	...	...	...	4.7	32.8
7	104.5- 91.0	7.5	76.2	...	...	...	3.5 <sub>4</sub>	38.6
8	91.0- 75.5	11.4	31.2	...	...	...	2.0	43.3
9	75.5- 57.7	18.8	5.6 <sub>6</sub>	...	...	...	1.7 <sub>1</sub>	30.9
10	57.5- 35.5	10.3	...	...	...	...	0.47	12.0
11	35.5- 8.0	...	...	...	...	...	0.06	0.59
12	8.0 ...	...	...	...	...	...	...	...

<sup>a</sup> Values in parenthesis are not shown in the corresponding excitation functions.

expected for a compound-nucleus mechanism is distorted in the higher energy ranges principally because of the recoil range of the products ( $P^{32}$ ,  $Cl^{34}$ ,  $Cl^{38}$ ). That is, the high-energy tail is probably due in part to a displacement of the peak anticipated for compound-nucleus formation and decay. However, consideration of range-energy relations<sup>7</sup> shows there can be little effect of recoil in the cases of the other nuclides observed in this study, since the available energy (for such products as  $Al^{28}$ ,  $Na^{24}$ , and other light residual nuclei) is insufficient to produce recoil ranges greater than one or two target foil thicknesses.

The energy resolution of the detector system (a  $3 \times 3$ -inch NaI(Tl) crystal; 400-channel pulse-height analyzer) employed in this work was 7.3% at 1.78 Mev and 9.3% at 0.84 Mev facilitating the identification of the gamma rays of interest and permitting an accurate half-life assignment to the gamma peaks at given energies. For this reason and because the gross beta decay observed by using an end-window gas flow proportional counter could be resolved accurately into its components, no chemical separations were performed.

A contribution to the activity observed for given residual nuclei by neutron-induced reactions was eliminated. This was accomplished by determining that no activity was present in the  $Al^{27}$  foils beyond the range of the full energy heavy-ion beams (65 mg/cm<sup>2</sup> for  $C^{12}$ ,

57.5 mg/cm<sup>2</sup> for  $N^{14}$ , and 50.5 mg/cm<sup>2</sup> for  $O^{16}$  at incident energies of  $10.5 \pm 0.2$  Mev/nucleon). If a neutron-induced contribution were significant, these activities would be observed in foils beyond this maximum range, as the range of fast neutrons is considerably greater than that of the heavy ions.

## DISCUSSION

The criteria used in interpreting the excitation functions as to reaction mechanism are based on the general considerations employed in light-particle-induced reaction studies.

Hence, mechanisms are crudely related to the excitation function shape and more exactly to the apparent threshold energy for the process in question. The shape of the excitation function anticipated for compound-nucleus formation and subsequent decay by evaporation cascade will exhibit a peaking in cross section. The peak should correspond to the most probable energy distribution for the evaporated fragments. In this study, the high-energy tail exhibited by the curves for such products as  $P^{32}$  and  $Cl^{34}$  arise, then, not only from the effect of finite recoil range (see results), but also from the existence of various modes of decay of the compound system forming the same residual nuclide. For example, in the  $P^{32}$  yield from  $C^{12}$  on  $Al^{27}$ , the most energetically favored mode of formation is that of evaporation of an alpha particle, deuteron, and proton from the compound system. At higher energies single-nucleon evaporation becomes energetically possible (see Table V). Hence, the cross section for the formation of the residual nuclide is a composite of several modes of formation resulting from the energy dependence of the several possible evaporation processes giving rise to this nuclide. However, the significant characteristic of marked energy dependence (resulting in peaking of the excitation function) is evident for the most probable type of evaporation cascade.<sup>8,9</sup>

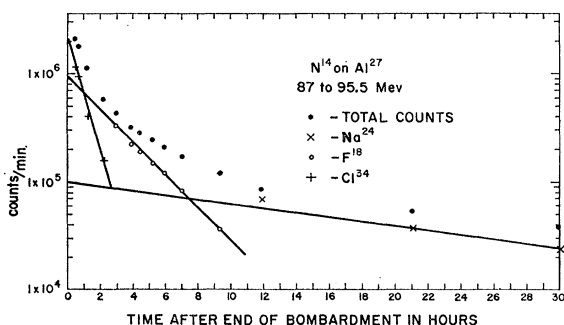
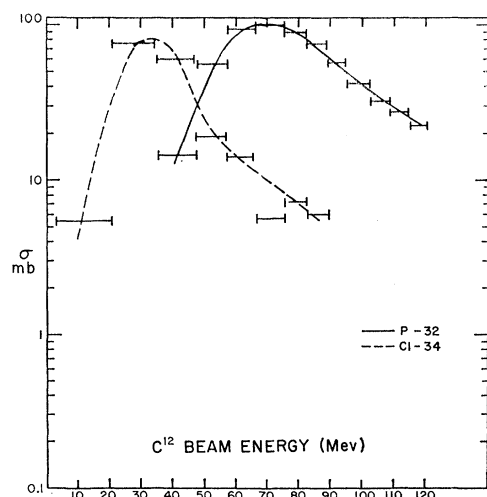


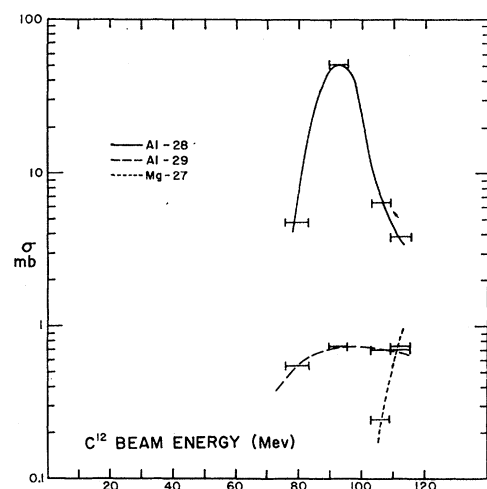
FIG. 1. Typical gross beta-decay curve observed in an Al foil after bombardment with 87- to 95.5-Mev  $N^{14}$  beam.

<sup>8</sup> R. Beringer and W. K. Knox, Phys. Rev. 121, 1195 (1961).

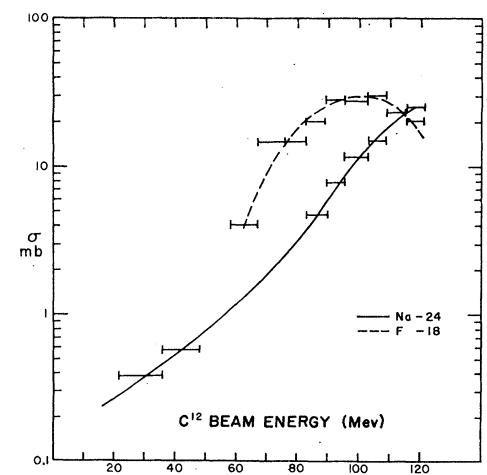
<sup>9</sup> R. Beringer (private communication).



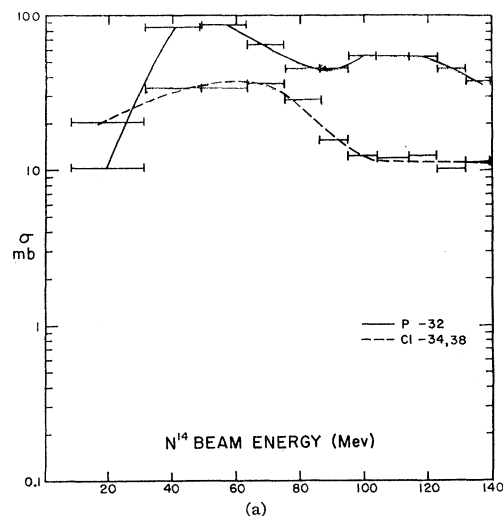
(a)



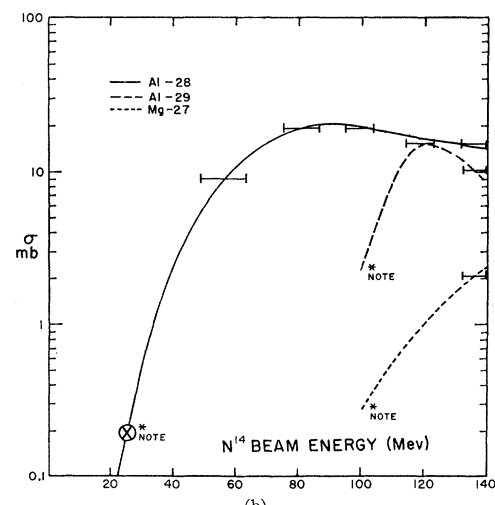
(b)



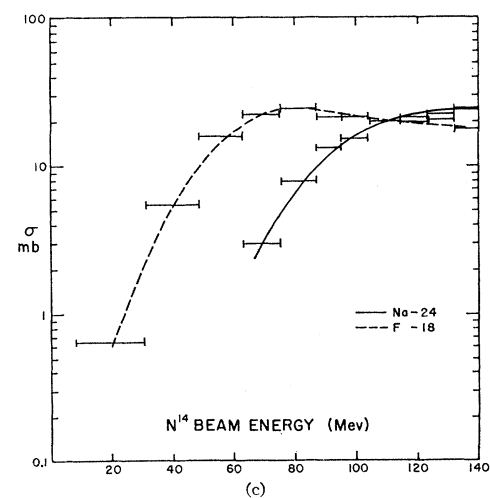
(c)



(a)



(b)



(c)

FIG. 2. Excitation functions for  $\text{C}^{12}$ -induced reactions on  $\text{Al}^{27}$ . The error bars represent the difference between beam energies on entering and leaving a given foil. (a) Excitation function for the formation of  $\text{P}^{32}$  and  $\text{Cl}^{34}$ . (b) Excitation function for the formation of  $\text{Al}^{28}$ ,  $\text{Al}^{29}$ , and  $\text{Mg}^{27}$ . (c) Excitation function for the formation of  $\text{Na}^{24}$  and  $\text{F}^{18}$ .

FIG. 3. Excitation function for  $\text{N}^{14}$ -induced reactions on  $\text{Al}^{27}$ . (a) Excitation function for the formation of  $\text{P}^{32}$  and  $\text{Cl}^{34,38}$ . (b) Excitation function for the formation of  $\text{Al}^{28}$ ,  $\text{Al}^{29}$ , and  $\text{Mg}^{27}$ . [Note the point in the  $\text{Al}^{28}$  data is that due to Webb *et al.* (reference 2); for specific information on the  $\text{Al}^{29}$  and  $\text{Mg}^{27}$  cross section, see Table III.] (c) Excitation functions for the production of  $\text{Na}^{24}$  and  $\text{F}^{18}$ .

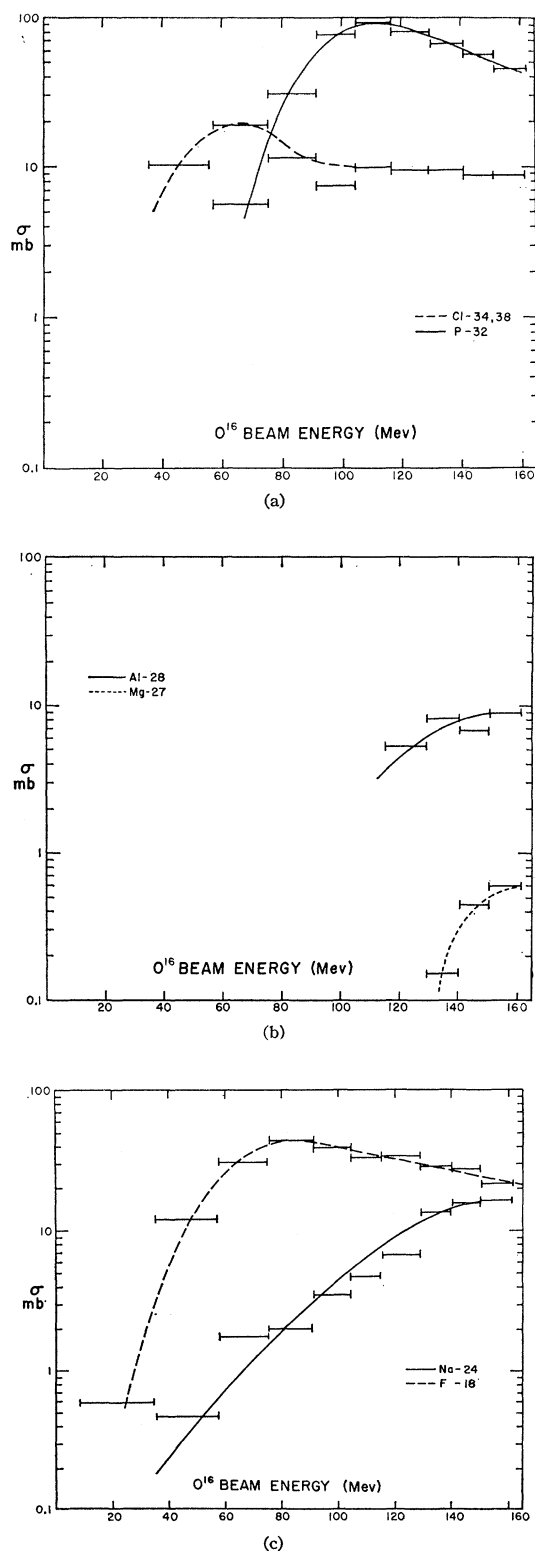


FIG. 4. Excitation functions for  $O^{16}$ -induced reactions on  $Al^{27}$ .  
 (a) Excitation function for the production of  $Cl^{34,38}$  and  $P^{32}$ .  
 (b) Excitation function for the production of  $Al^{28}$  and  $Mg^{27}$ .  
 (c) Excitation function for the production of  $Na^{24}$  and  $F^{18}$ .

The excitation functions for direct interaction products should exhibit little tendency toward the marked energy dependence (resulting in sharp peaking) found for the compound-nucleus mechanism. Recoil of the residual nuclides produced via the direct process and for nuclides of masses similar to, or less than, that of the target formed by either mechanism will be negligible. For example the absence of the high-energy tail for the  $Al^{28}$  yield from  $O^{16}$  on  $Al^{27}$ , and the yields of  $F^{18}$  and  $Na^{24}$  illustrate this point.

Tunneling<sup>10-13</sup> and grazing collision processes,<sup>14</sup> by definition are reactions proceeding below or just above the Coulomb barrier, and will be considered only in those cases where the low-energy limitations of this study permit.

### $C^{12}$ -Ion-Induced Reactions

The shape of the excitation function indicates that the formation of  $P^{32}$ ,  $Cl^{34}$ , and  $Al^{28}$  are a result of compound-nucleus formation and decay. As noted above, at higher beam energies it is possible that several modes of production, and/or energy distribution of evaporated nucleons, result in the tail exhibited by the excitation functions found for  $P^{32}$  and  $Cl^{34}$ . Since the peaking in the  $Al^{28}$  yield occurs at relatively high beam energies with respect to the Coulomb barrier, such processes as tunneling or grazing collisions probably contribute little to the yield of this nuclide in the  $C^{12}$ - $Al^{27}$  system.

The data indicate that probably both  $F^{18}$  and  $Al^{29}$  were formed with a marked contribution from the compound-nucleus process, although the broad peaking (as compared to that for  $Al^{28}$ ) would suggest that a contribution from a direct-interaction mode of formation could be significant (e.g., 2-neutron pickup in the case of  $Al^{29}$ ). The yield of  $Al^{29}$  from the compound system would be expected to be less than that of  $Al^{28}$  on the basis of level density considerations. However, the very large decrease in relative yield as compared to  $Al^{28}$  would not seem justifiable on this basis alone.

While sufficient data are not available to assign the production of  $Mg^{27}$  to any specific reaction mechanism, the apparent threshold energy would indicate that this residual nuclide is formed principally through a compound-nucleus process.

The yield of  $Na^{24}$  appears to exhibit the characteristics of a direct interaction mechanisms at the lower energies (energy below the threshold for the evaporation of nucleons from the compound system). At higher energies, the changes in slope of the excitation function would seem to indicate that the compound-nucleus process contributes to the yield to a marked

<sup>10</sup> J. A. McIntyre, T. L. Watts, F. C. Jobs, Phys. Rev. **119**, 1131 (1960).

<sup>11</sup> G. Breit, M. Hitlull, R. C. Gluckstern, Phys. Rev. **87**, 74 (1952).

<sup>12</sup> G. Breit, M. E. Ebel, Phys. Rev. **103**, 679 (1956).

<sup>13</sup> G. Breit, M. E. Ebel, Phys. Rev. **104**, 1030 (1956).

<sup>14</sup> R. Kaufman and R. Wolfgang, Phys. Rev. **121**, 206 (1961).

TABLE V.  $Q$  values<sup>a</sup> for the formation of the residual nuclei observed.

$\text{N}^{14} + \text{Al}^{27}$		$\text{C}^{12} + \text{Al}^{27}$		$\text{O}^{16} + \text{Al}^{27}$	
Products	$-Q(\text{Mev})$	Products	$-Q(\text{Mev})$	Products	$-Q(\text{Mev})$
$\text{Cl}^{38} + 3p$	6.41	...	...	$\text{Cl}^{38} + 4p + 1n$	29.28
$\text{Cl}^{34} + 1\alpha + 1p + 2n$	15.79	$\text{Cl}^{34} + 1\alpha + 1n$	3.30	$\text{Cl}^{34} + 2\alpha + 1n$	10.46
$\text{Cl}^{34} + 3p + 4n$	44.08	$\text{Cl}^{34} + 2p + 3n$	31.46	$\text{Cl}^{34} + 4p + 5n$	66.97
$\text{P}^{32} + 2\alpha + 1p$	2.17	$\text{P}^{32} + 1\alpha + 2p + 1n$	17.59	$\text{P}^{32} + 2\alpha + 2p + 1n$	25.10
$\text{P}^{32} + 5p + 4n$	58.75	$\text{P}^{32} + 4p + 3n$	46.26	$\text{P}^{32} + 6p + 5n$	81.62
$\text{Al}^{28} + 3\alpha + 1p$	12.05	$\text{Al}^{28} + 2\alpha + 2p + 1n$	27.63	$\text{Al}^{28} + 3\alpha + 2p + 1n$	34.96
$\text{Al}^{28} + 7p + 6n$	96.81	$\text{Al}^{28} + 6p + 5n$	79.78	$\text{Al}^{28} + 8p + 7n$	120.06
$\text{Al}^{29} + 2\alpha + 3p + 1n$	30.94	$\text{Al}^{29} + 2\alpha + 2p$	18.45	$\text{Al}^{29} + 3\alpha + 2p$	25.61
$\text{Al}^{29} + 7p + 5n$	87.43	$\text{Al}^{29} + 6p + 4n$	74.95	$\text{Al}^{29} + 8p + 6n$	110.36
$\text{Mg}^{27} + 3\alpha + 2p$	21.60	$\text{Mg}^{27} + 2\alpha + 3p + 1n$	37.39	$\text{Mg}^{27} + 3\alpha + 3p + 1n$	44.55
$\text{Mg}^{27} + 8p + 6n$	106.45	$\text{Mg}^{27} + 7p + 5n$	93.68	$\text{Mg}^{27} + 9p + 7n$	120.21
$\text{Na}^{24} + \text{N}^{13} + p$	13.69	...	...	...	...
$\text{Na}^{24} + \text{F}^{17}$	7.88	...	...	...	...
$\text{Na}^{24} + 4\alpha + 1p$	22.92	$\text{Na}^{24} + 3\alpha + 2p + 1n$	38.89	$\text{Na}^{24} + 4\alpha + 2p + 1n$	45.86
$\text{Na}^{24} + 9p + 8n$	135.92	$\text{Na}^{24} + 8p + 7n$	123.44	$\text{Na}^{24} + 10p + 9n$	158.85
$\text{F}^{18} + \text{Na}^{23}$	5.70	...	...	...	...
$\text{F}^{18} + 5\alpha + 1p + 2n$	41.47	$\text{F}^{18} + 5\alpha + 1n$	38.28	$\text{F}^{18} + 6\alpha + 1n$	45.44
$\text{F}^{18} + 11p + 12n$	191.92	$\text{F}^{18} + 10p + 11n$	179.53	$\text{F}^{18} + 12p + 13n$	214.95

<sup>a</sup> V. A. Kravtsov, *Uspekhi Fiz. Nauk*, **65**, (3), 451 (1958); mass table used for the calculation of the  $Q$  values.

degree over that of direct interaction. A more exact analysis is prohibited by the high-energy limitation of the experiment.

### $\text{O}^{16}$ Induced Reactions

Both the formation of  $\text{P}^{32}$  and the composite  $\text{Cl}^{34}$ - $\text{Cl}^{38}$  can be attributed to compound-nucleus formation and decay based on the shapes of the excitation functions. The high-energy tail in the  $\text{Cl}^{34}$  and  $\text{Cl}^{38}$  yield is principally due to the inability to resolve the two  $\text{Cl}$  gamma or beta rays. The yields of both  $\text{Cl}^{34}$  and  $\text{Cl}^{38}$  should exhibit peaking characteristics of the compound-system mechanism. In addition the apparent threshold energies agree with the calculations shown in Table V.

Insufficient data are available in this study to determine the magnitude of the contributions from the various mechanisms that could give rise to  $\text{Al}^{28}$  and  $\text{Mg}^{27}$  formation resulting from  $\text{O}^{16}$  irradiations. However, the gradual slope of the  $\text{Al}^{28}$  excitation function seems to suggest a contribution by a direct neutron pickup process by the target nucleus. The magnitude of the cross section and nature of the gamma spectrum of this nuclide did not permit excitation function assignments at the lower beam energies.

The shape of the excitation function strongly infers that both  $\text{F}^{18}$  and  $\text{Na}^{24}$  are formed through a direct-interaction mechanism. The  $\text{F}^{18}$  yield (at energies below that required for the evaporation of particles from the compound nucleus) is suggestive of a deuteron pickup by the incident projectile, while the  $\text{Na}^{24}$  excitation function would seem to predict direct knockout, or pickup by the projectile, of a  $\text{He}^3$  cluster associated with the target nucleus.

### $\text{N}^{14}$ Induced Reactions

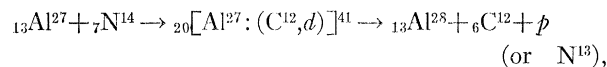
The excitation function found for  $\text{P}^{32}$  and  $\text{Cl}^{34-38}$  composite in the  $\text{N}^{14}$  bombardments on  $\text{Al}^{27}$  indicates

a compound-nucleus formation and decay mechanism. The two peaks observed for  $\text{P}^{32}$  yield may result from two independent modes of decay of the compound-nucleus system; one involves primarily particle emission and the other (at lower energies) involves  $\alpha$ -particle evaporation from the compound nucleus. (See Table V.)

Although the data are limited to only a few points, the shape of the excitation functions indicates that at the higher energies the compound-nucleus mechanism is the major mode of the formation of  $\text{Al}^{29}$  and probably a large portion of the  $\text{Mg}^{27}$  production. However, Pinajian<sup>5</sup> has pointed out that the low-energy yield (thick target cross section at 27.6-Mev  $\text{N}^{14}$ -110  $\mu\text{b}$ ) seems to be characteristic of an exchange-transfer reaction, which is analogous to the  $\text{Li}^6$ - $\text{Al}^{27}$  system.<sup>6</sup> The  $\text{Al}^{29}$  yield would most certainly have a reasonable contribution from a direct two-neutron pickup by the target. However the limitations of the experiment prohibit further conjecture on this point.

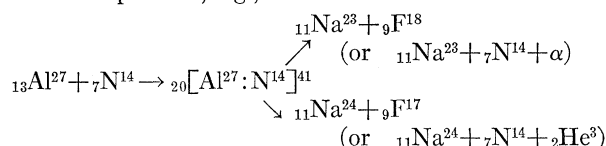
The excitation function for the yield of  $\text{Al}^{28}$  shows that a direct-interaction mode of production is predominant. A comparison with data previously reported<sup>3,4</sup> gives good agreement with the excitation function observed at low energies. However, at higher energies (above 5 Mev/nucleon) the  $\text{N}^{13}$  yield from the  $\text{Al}^{27}$ - $\text{N}^{14}$  system reported by Volkov<sup>8</sup> is less than that of  $\text{Al}^{28}$  observed in the current experiment. This apparent disagreement may be explained on the basis of several mechanistic approaches. At low energies (below or at the barrier) the predominant reaction mechanism is that of a neutron tunneling,<sup>9-12</sup> giving rise to similar yields for both  $\text{N}^{13}$  and  $\text{Al}^{28}$ . However, at higher energies contributions to the  $\text{Al}^{28}$  yield by mechanisms not producing  $\text{N}^{13}$  may become significant (e.g., compound-nucleus formation and decay) in addition to the stripping process producing  $\text{N}^{13}$ . Furthermore, if a reaction-intermediate<sup>6</sup> mechanism

is envisioned, i.e.,



both  $\text{N}^{13}$  and  $\text{C}^{12} + p$  could be formed, contributing to the observed yield of  $\text{Al}^{28}$  while decreasing the cross section for the  $\text{N}^{13}$  formation as such.

Both the shape of the excitation functions and the apparent threshold energies (as compared to that needed for compound-nucleus decay, Table V) indicate the yield of both  $\text{F}^{18}$  and  $\text{Na}^{24}$  can be attributed almost entirely to a direct-interaction mechanism. This process would involve the pickup of  $\text{He}^4$  by the projectile from the target material forming  $\text{F}^{18}$ , and either pickup by the  $\text{N}^{14}$  or direct knockout of a  $\text{He}^3$  cluster in the case of  $\text{Na}^{24}$ . The formation of both these radio nuclides (as well as  $\text{Al}^{28}$ ,  $\text{Mg}^{27}$ , and  $\text{Al}^{29}$ ) would be enhanced by the formation of a reaction intermediate in which the exchange of several nucleons or nucleon clusters<sup>15,16</sup> would be possible, e.g.,



<sup>15</sup> K. Wildenmuth and Th. Kanellopoulos, European Organization for Nuclear Research Report, Geneva, CERN-59-23, 1959 (unpublished).

<sup>16</sup> D. H. Wilkinson, *Phil. Mag.* **4**, 215 (1959).

## CONCLUSIONS

The over-all effect of the deuteron structure of  $\text{N}^{14}$  is evident from the shapes of the excitation functions as compared with those found for the alpha-particle nuclei  $\text{O}^{16}$  and  $\text{C}^{12}$ . In particular the direct-interaction mechanism suggested by the excitation function for the formation of  $\text{Al}^{28}$  by  $\text{N}^{14}$  (stripping mechanism) in contrast with the shapes found for  $\text{Al}^{28}$ ,  $\text{O}^{16}$ , and  $\text{C}^{12}$ -induced production seems to be indicative of the deuteron-type cluster (with a weakly bound neutron) in  $\text{N}^{14}$ , similar to that observed by the authors for  $\text{Li}^6$ -induced reactions.<sup>6</sup>

The competition between the various reaction mechanisms proposed should exhibit marked energy dependence. The experiment as performed did not possess energy resolutions sufficient to permit observation of subtle variations in cross section over small energy increments.

Work is in progress at this laboratory which will permit the comparison between the activation excitation functions and those established by direct particles and heavy-fragment observation (e.g.,  $de/dx$  vs  $E$  detections).<sup>17,18</sup>

## ACKNOWLEDGMENTS

We would like to thank Professor D. A. Bromley and Professor R. Wolfgang for helpful discussions and the crew of the Heavy Ion Accelerator for their cooperation. In addition we thank Mr. Martin Sachs for helping in accumulating the gamma-ray data.

<sup>17</sup> D. A. Bromley (private communication).

<sup>18</sup> C. E. Anderson (private communication).